Available online at www.sciencedirect.com
SCIENCE DIRECT®
Journal of Organometallic Chemistry 683 (2003) 209–219
Journal of Organometallic Chemistry
www.elsevier.com/locate/jorganchem

Propylene bulk phase oligomerization with bisiminepyridine iron complexes in a calorimeter: mechanistic investigation of 1,2 versus 2,1 propylene insertion

Sebastian Thomas Babik, Gerhard Fink *

Max-Planck-Institut für Kohlenforschung, Kaiser-Wilhelm-Platz 1, 45470 Mulheim an der Ruhr, Germany

Received 27 March 2003; accepted 28 June 2003

Dedicated to Prof. M.T. Reetz on the occasion of his 60th birthday

Abstract

Iron(II) complexes were synthesized with bisiminepyridine ligands of low steric demand. Activation with modified-methylaluminoxane (25 mol.% isobutyl groups) generated very active catalysts for propylene oligomerization. The oligomerizations were carried out in liquid propylene in a heat flow calorimeter. The oligomers were separated by preparative gas chromatography and the dimers and trimers analyzed using analytical gas chromatography, ^{1}H-NMR- and ^{13}C-NMR-spectroscopy. With knowledge of the dimer and trimer structure, we were able to establish a mechanistic pathway for propylene insertion and obtained knowledge about the iron alkyl species involved. Analysis of the various dimers formed allowed us to determine the percentage of 1,2 versus 2,1 propylene insertions. Considering the same iron alkyl species with ligands of different steric demand, a change in the probabilities for 1,2 versus 2,1 propylene insertions can be observed. With this knowledge, the catalyst behavior for ligands of varying steric demand can be predicted.

Keywords: Bisiminepyridine iron complex; Sterical demand of the ligand system; Propylene oligomerization; Propylene dimers; 1,2 and 2,1 propylene insertion

1. Introduction

One goal of our research group is to learn more about the mechanisms of polymerization reactions, which can lead us to control these reactions by tuning the steric and electronic properties of the reactive center. There persists great industrial interest in producing polymeric materials that satisfy the consumer needs exactly. The aim of our research is to produce these 'tailor-made-polymers'. In general it is possible to adjust the polymer properties by changing the ligand structure or varying the reaction conditions, temperature, monomer pressure and co-catalyst ratio [1–4]. It is an indispensable precondition to know as much as possible about the propagation and termination steps of the polymerization reaction. If we have more information about these steps we know in which direction we have to adjust for instance the bulkiness of a substituent, the strength of an electronic withdrawing group or the nature of the co-catalyst. Our group has made mechanistic investigations in metallocene catalyzed propylene polymerizations and norbornene–ethylene copolymerizations [5,6].

Recently there has been growing academic and industrial interest in polymerization catalysts based on bisiminepyridine complexes with iron. This type of catalysts was developed and investigated by Brookhart and co-workers and Gibson and co-workers in the late 1990s [7,8]. It is known that they are very active in ethylene and propylene polymerization with activation by methylaluminoxane, modified-methylaluminoxane (MMAO) or $Ph_3C[B(C_6F_5)_4]$ and AlR_3 [9–16,21]. We recently published a paper describing a catalytic cycle that involves an iron hydride species, which is the result

* Corresponding author. Tel.: +49-208-306-2240; fax: +49-208-306-2980.
E-mail address: fink@mpi-muelheim.mpg.de (G. Fink).

0022-328X/03/$ - see front matter © 2003 Elsevier B.V. All rights reserved.
doi:10.1016/S0022-328X(03)00670-3

of a β-H-elimination [17]. This hydride is in our opinion the result of a β-H-elimination. There is also the possibility of a transfer reaction to the monomer as discussed in the theoretical works by Ziegler and Morokuma [22,23]. More experiments are necessary to determine whether the termination step is a transfer reaction or a β-H-elimination.

To further analyze the mechanism of propylene polymerization with bisiminepyridine iron complexes, it would be ideal to isolate an iron alkyl species to further understand the nature of the inserting and propagating iron alkyl species. The problem being that it has not been possible to isolate such a species. Thus, we decided to regard this problem from another perspective and isolate dimers and trimers of propylene produced by less sterically demanding iron bisiminepyridine complexes. After identifying the dimer or trimer it is possible to extrapolate the nature of the previous iron alkyl from which the dimer or trimer was formed.

After producing polymer when using bulky catalysts it was surprising to find eight different dimers and at least seven different trimers, when using a less sterically demanding catalyst. This indicates a very complicated system of insertion and subsequent eliminations. For example, some iron alkyls prefer to insert propylene in 1,2 fashion, some in a 2,1 fashion, some do not insert propylene at all. We also found a high fraction of 2-olefins which show *E*/*Z* isomerization. In this manuscript we report the product distribution of three different iron bisiminepyridine catalysts and present our conclusions concerning the nature of the iron alkyl species involved and the influence of the steric properties of the ligands on the reactivity of those alkyl species.

2. Experimental

2.1. General considerations

The handling of water- and air-sensitive compounds was performed under an argon atmosphere using Schlenk techniques.

2.2. Materials

Methanol was dried over CaH_2/Mg and distilled. Toluene was distilled from sodium. THF was distilled from MgH_2. 2,6-Diacetylpyridine, aniline, 2,4-dimethylaniline, 2-ethylaniline, 97% formic acid and $FeCl_2$ were purchased from Aldrich and used without further purification. MMAO (7 wt.% solution in toluene, 25% isobutyl groups) was purchased from Texas Alkyls Inc. Propylene (99.5%) was purchased from Messer-Griesheim and used without further purification.

2.3. Synthesis of 2,6-bis[1-(phenylimino)ethyl]-pyridine (L1) [18]

2,6-Diacetylpyridine (1.14 g, 7.0 mmol) was dissolved in 15 ml of methanol in a 50 ml round-bottom flask. Aniline (1.86 g, 20.0 mmol) was added. Four drops of 97% formic acid were added and the clear, orange solution was allowed to stir in the sealed flask at ambient temperature for 5 h. After stirring the resultant pale yellow solid precipitate was collected by filtration, washed with cold methanol and dried. The yield was 1.86 g (85%) of pure ligand.

^{1}H-NMR ($CDCl_3$): $\delta = 8.23$–8.26 (d, 2, py-H_m); 7.78–7.83 (t, 1, py-H_p); 7.28–7.34 (t, 4, H_{aryl}); 7.02–7.08 (t, 2, H_{aryl}); 6.76–6.79 (d, 4, H_{aryl}); 2.34 (s, 6, N=CCH_3).

2.4. Synthesis of 2,6-bis[1-(2,4-dimethylphenylimino)ethyl]-pyridine (L2) [8,13]

2,6-Diacetylpyridine (1.25 g, 7.7 mmol) was dissolved in 20 ml of methanol in a 50 ml round-bottom flask. 2,4-Dimethylaniline (2.88 g, 22.0 mmol) was added. Five drops of 97% formic acid were added and the clear, orange solution was allowed to stir in the sealed flask at ambient temperature for 15 h. After stirring overnight the resultant yellow solid precipitate was collected by filtration, washed with cold methanol and dried. The yield was 2.04 g (72%) of pure ligand.

^{1}H-NMR ($CDCl_3$): $\delta = 8.30$–8.33 (d, 2, py-H_m); 7.81–7.86 (t, 1, py-H_p); 6.92–6.98 (m, 2, H_{aryl}); 6.78–6.79 (m, 2, H_{aryl}); 6.49–6.53 (d, 2, H_{aryl}); 2.26 (s, 6, N=CCH_3); 2.14 (s, 6, arylCH_3); 2.02 (s, 6, arylCH_3).

2.5. Synthesis of 2,6-bis[1-(2-ethylphenylimino)ethyl]-pyridine (L3)

2,6-Diacetylpyridine (1.19 g, 7.3 mmol) was dissolved in 15 ml of methanol in a 50 ml round-bottom flask. 2-Ethylaniline (2.49 g, 19.0 mmol) was added. Four drops of 97% formic acid were added and the clear, orange solution was allowed to stir in the sealed flask at room temperature (r.t.) for 15 h. After stirring overnight the resultant pale yellow solid precipitate was collected by filtration, washed with cold methanol and dried. The yield was 1.86 g (69%) of pure ligand.

^{1}H-NMR ($CDCl_3$): $\delta = 8.39$–8.42 (d, 2, py-H_m); 7.86–7.93 (t, 1, py-H_p); 7.18–7.27 (m, 4, H_{aryl}); 7.06–7.11 (m, 2, H_{aryl}); 6.66–6.69 (d, 2, H_{aryl}); 2.48–2.56 (quart., 4, arylCH_2Me); 2.37 (s, 6, N=CCH_3); 1.12–1.18 (t, 6, arylCH$_2$CH_3).

2.6. Synthesis of the iron complexes (C1–C3) [7–16]

Dry $FeCl_2$ (one equivalent) in 20 ml dry THF was stirred under an argon atmosphere in a 100 ml flame-

dried two-neck-flask. A solution of Ligand L (1.05 equivalent) in 25 ml dry THF was added slowly at r.t. via a dropping funnel. The brown suspension of $FeCl_2$ turned immediately into a blue color. The mixture was then stirred under argon for one additional hour. Then pentane was added to the blue suspension and the solid was filtered and dried under argon. The light-blue complex was isolated in near quantitative yield. The complexes were analyzed using ESI mass spectroscopy, where the molecular peak of the iron complex and the molecular peak of the corresponding ligand were the only peaks detected.

2.7. Oligomerization process

All polymerizations were carried out in a 1.8 l high-pressure steel reactor using the Mettler RC1 reaction calorimeter [19,20]. The reactions were performed in the isothermal mode using an anchor stirrer (250 rpm) under the vapor pressure of liquid propylene at the corresponding temperature. First 1 ml of the MMAO solution was added via syringe to the reactor as a scavenger. One liter of propylene was added to the reactor by condensation, measured by the loss in the propylene supply gas bottle. The reactor was then heated to the reaction temperature. A modification to the standard Mettler RCI is a separate thermostatically controlled bath used to circulate maintain the reactor head 2 °C above the reaction temperature to avoid condensation and to minimize heat losses. The catalyst in a suspension of 5 ml anhydrous toluene was injected into the reactor immediately followed by another solution of 0.5 ml of MMAO in 4.5 ml of toluene using argon pressure. The injection system has been thermostated to the temperature of the reactor by means of the thermostatically controlled bath in order to minimize an initial temperature disturbance. The polymerizations were stopped by injection of water. Throughout the entire reaction, temperatures, pressure and heat was recorded. With this data, it is possible to determine a kinetic profile for the reaction. After each experiment the remaining propylene is vented. The organic phase, which consists usually of more than 95% oligomers and 5% of toluene is separated from the aqueous phase containing catalyst and the decomposed MMAO. The organic phase is diluted with toluene and analyzed directly using GC and preparative GC.

2.8. Oligomer separation and characterization

The oligomers were analyzed using a GC with a Carlo Erba 4100 equipped with a 60 m RTX-1 column (0.25 μm) and a FID. Identification of the dimers and trimers necessitated isolation of each isomer. This was performed using multidimensional preparative gas chromatography, based on a Shimadzu Tandem-GC 14A. The use of multidimensional separation in coupled columns with techniques such as 'peak cutting' and 'back flushing' enables this instruments to separate larger amounts of purified substances.

^{1}H-NMRs (300 MHz) and ^{13}C-NMRs (75.5 MHz) were carried out using a Bruker DPX-300 spectrometer and $CDCl_3$ as solvent.

3. Results and discussion

Fig. 1 shows the catalysts synthesized in this work. The main focus of this work will be on the product distribution of the oligomers in order to draw conclusions about the iron alkyls that are taking part in the reaction. Fig. 2 is a GC plot of a typical oligomeric mixture obtained with catalyst **1**. In this figure, the region of the dimers and trimers has been enlarged and will be the focus henceforth.

The identification of di- and trimers was performed with ^{1}H- and ^{13}C-NMR after separation using preparative gas chromatographically. In some cases it was not possible to separate the substances using this method. In the enlarged analytical plot (Fig. 2) two or even three substances are assigned to a single peak such as peak 26–28 in the C9-fraction. However, it was possible to identify the different olefinic groups because the 1-olefin and the 2-olefin protons have distinct signals (Fig. 3).

It was also possible to identify *E*- and *Z*-isomers. It was possible to compare synthesized olefins using reference olefins with known configuration. As shown in Fig. 4, it is possible to differentiate between *E*- and *Z*-isomers using ^{1}H-NMR. The *Z*-isomers show slightly broader signals in the olefinic region and the shape and chemical shift of the 'D-group' differs. The *E*-isomer is slightly below 2 ppm and the *Z*-isomer above 2 ppm, making it possible to distinguish between the two isomers easily.

Once the dimers and trimers have been correctly identified, it is possible to proceed with the mechanistic considerations. Fig. 5 shows the isomer distribution of the C6-fraction at three different temperatures produced with catalyst **1**.

With increasing temperature, there is an increase in the percentage of dimer **1** (4-methyl-1-pentene) while the amount of dimer **4** (*E*-4-methyl-2-pentene) is decreasing. On the other hand, the percentage of dimer **3** (*Z*-4-methyl-2-pentene) is increasing only slightly. The increasing temperature favors the formation of the 1-olefin and the *Z*-isomer of the 2-olefin. Furthermore, the temperature has almost no effect on the distribution of the other dimers. The percentage of the dimers **1**–**8** is constant over the studied temperature range.

Scheme 1 illustrates all the olefins and corresponding iron alkyls that occur in this reaction. Percentage near the arrows indicates whether a 1,2 or 2,1 propylene

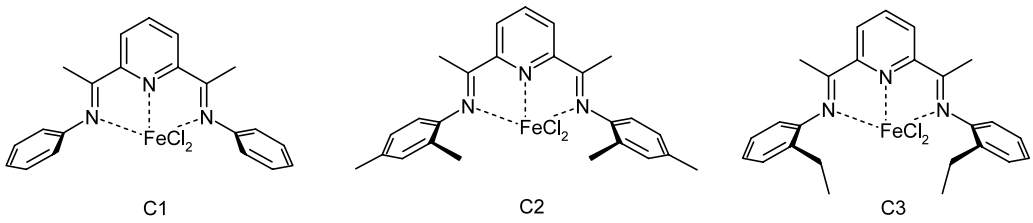

Fig. 1. Complexes in study.

insertion occurs. The given numbers only relate to the dimer distribution and neglect that some species are still involved in the growth to trimers and so on.

The three latter dimers **1**, **3** and **4**, result from the same iron alkyl, shown in Scheme 1 in the bottom right. From this position there are two possible directions for the chain termination step. One towards the short branch which forms the 1-olefin (**1**) and the other direction towards the longer branch which form the two 2-olefins (**2** and **3**). In the case of the dimers **6** (1-hexene), **7** (*E*-2-hexene) and **8** (*Z*-2-hexene), one iron alkyl leads to all three dimers. Concerning dimers **2** (2,3-dimethyl-1-butene) and **5** (2-methyl-1-pentene) the first species is a primary iron alkyl where only one direction is possible for the termination, resulting in a vinylidene double bond.

In the middle of Scheme 1 is the proposed starting hydride species [17]. From this species there are two possibilities for a propylene insertion. Moving left in Scheme 1 (white arrow), the propylene inserts in a 1,2-arrangement and forms the iron-*n*-propyl species. From this species there are again two possible routes for an incoming propylene: the 1,2- or the 2,1-insertion. Analyzing the formed dimers, it is possible to conclude that there is a 50 to 50 probability for a propylene insertion via a 1,2 or a 2,1 step.

A different situation is found when following the black arrow to the right of the hydride and starting with a 2,1 propylene insertion. The formed iron isopropyl species favors the subsequent 2,1-insertion by more than 90% about the 1,2-insertion. The iron alkyl formed after two 2,1 propylene insertions is the dominant species for the further growth to tri- and higher oligomers. This is confirmed by the distribution of the C9 fraction seen in Fig. 2. The amount of substituted trimers is higher than the more linear trimers. We can say it is more likely that the propylene inserts in a 2,1- than in a 1,2-arrangement both in the iron hydride and the iron alkyl when we use the least sterically demanding catalyst **1**.

What happens when the sterical demand of the system is increased by using catalyst **2**? Here there is a methyl group in the *ortho* position of the phenylimin. In Fig. 6 is the distribution of the C6 fraction produced with catalyst **2** at different temperatures.

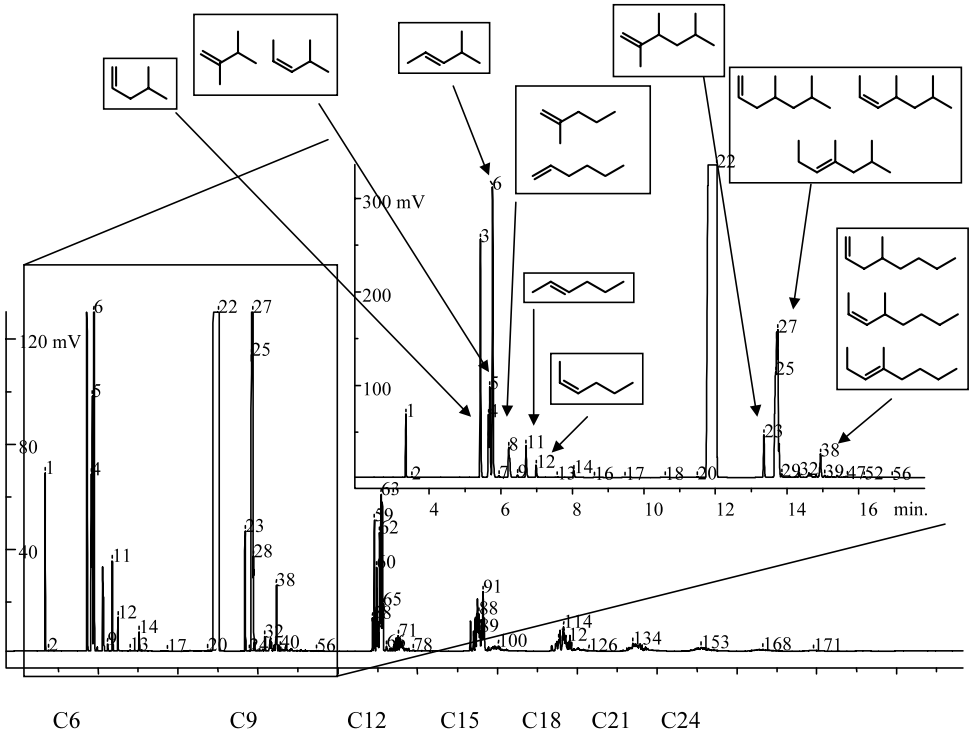

Fig. 2. Propylene oligomer distribution and identified dimers and trimers; catalyst **1**.

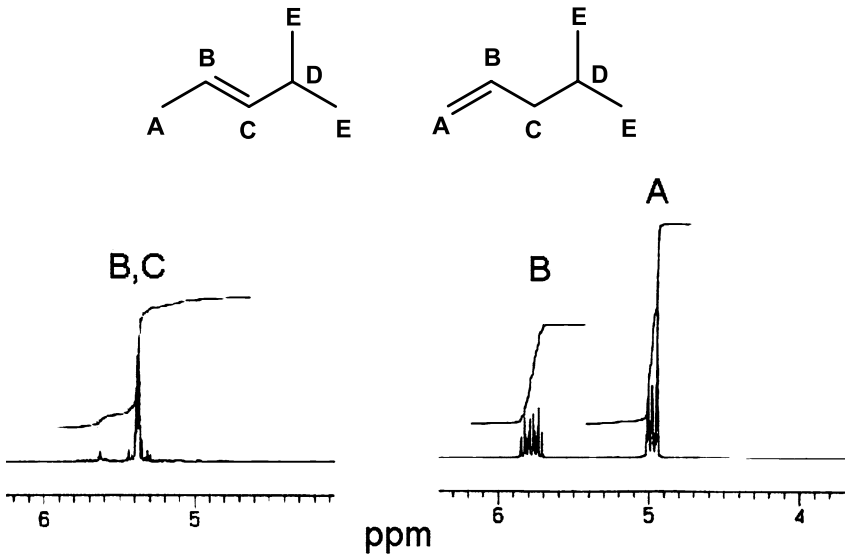

Fig. 3. Comparison of olefinic end groups, ^{1}H-NMR of 1- and 2-olefinic groups.

Catalyst **2** gives a completely different dimer distribution compared to catalyst **1**. In this case, hexenes **6**, **7** and **8** are the most populated dimers and no longer the methyl pentenes. Catalyst **2** also shows different temperature behavior, increasing temperature results in an increase in the amount of the dimers **1**, **3** and **4** formed. When catalyst **1** was used, there was also an increase in the dimers **1** and **3**, but a decrease in dimer **4**. This difference in the termination behavior must relate to the slightly higher sterical demand in the ligand sphere of catalyst **2**. The distribution of the linear hexenes **6**, **7** and **8** shows that the amount of 1-hexene (**6**) remains constant while the amount of dimer **7** (*E*-2-hexene) and **8** (*Z*-2-hexene) is decreasing. Dimer **2** and **5** distributions are not effected changing the temperature from 20 to 40 °C.

In Scheme 2, the mechanistic pathway for catalyst **2** is shown. Comparing the behavior of catalyst **2** and catalyst **1** there is an interesting shift in the mechanism. The cycle begins again with the Fe–H species in the middle of Scheme 2. The higher sterical demand of the ligand system leads to a 69:31 favored 1,2 propylene insertion (white arrow) in the iron hydride instead of a 88:12 favored 2,1 insertion in the case of catalyst **1**. Concerning the first insertion of propylene into the Fe–H bond the reason for this change must be the sterical effect of the ligand system, because this is the only difference between the two catalysts. Considering the second propylene insertion after a previous 2,1 insertion (black arrow) the same ratio is observed as with catalyst **1**. However, upon the second insertion after a 1,2-insertion (white arrow) there is a great change in the 2,1 insertion in the iron-*n*-propyl species from a 68:32 ratio in the case of catalyst **1** to a 91:9 ratio for catalyst **2**. It is quite interesting that the ratio is almost the same as 93:7 ratio after the first 2,1 insertion. There must be a combined sterical demand of the ligand system and the growing chain at the iron center, causing the increase in the percentage of 2,1 insertions. In the case of the less sterically demanding catalyst **1,** the *n*-propyl group after the first 1,2 propylene insertion can arrange in such a way that there is no preference for either a 1,2- or a 2,1-insertion. The two methyl groups of the iron isobutyl species have a higher sterical demand than the linear *n*-propyl group, causing a more hindered iron center. The higher sterically demanding catalyst **2** prevents the rearrangement of the linear *n*-propyl group and the sterical demand nears this of the isopropyl group. With catalyst **2**, there seems to be no difference for the incoming propylene between an iron-*n*-propyl and an iron-isopropyl group.

With a higher sterical demand in the ligand system there is an increasing preference for the first 1,2 propylene insertion and an increasing tendency for the second 2,1-insertion is observed. The next system investigated was the sterically most demanding, a *ortho*-ethyl substituted catalyst **3**. Fig. 7 shows the distribution of the C6 fraction obtained with this catalyst.

Catalyst **3** follows the same general trend in dimer distribution observed with catalyst **1** and **2**. With higher sterical demand of the ligand system, more hexenes (**6**, **7** and **8**) and fewer substituted pentenes (**1**, **3** and **4**) are formed. Dimers **2** and **5** were not detected at all. The trend in oligomer distribution with changing temperature is similar to catalyst **2**.

Scheme 3 is the mechanistic pathway for catalyst **3**.

Beginning with the iron hydride species, almost the same probabilities for a 1,2- and a 2,1-arrangement for the initial propylene insertion are observed as with catalyst **2**. The biggest difference between the two catalysts is found in the second step. In the case of

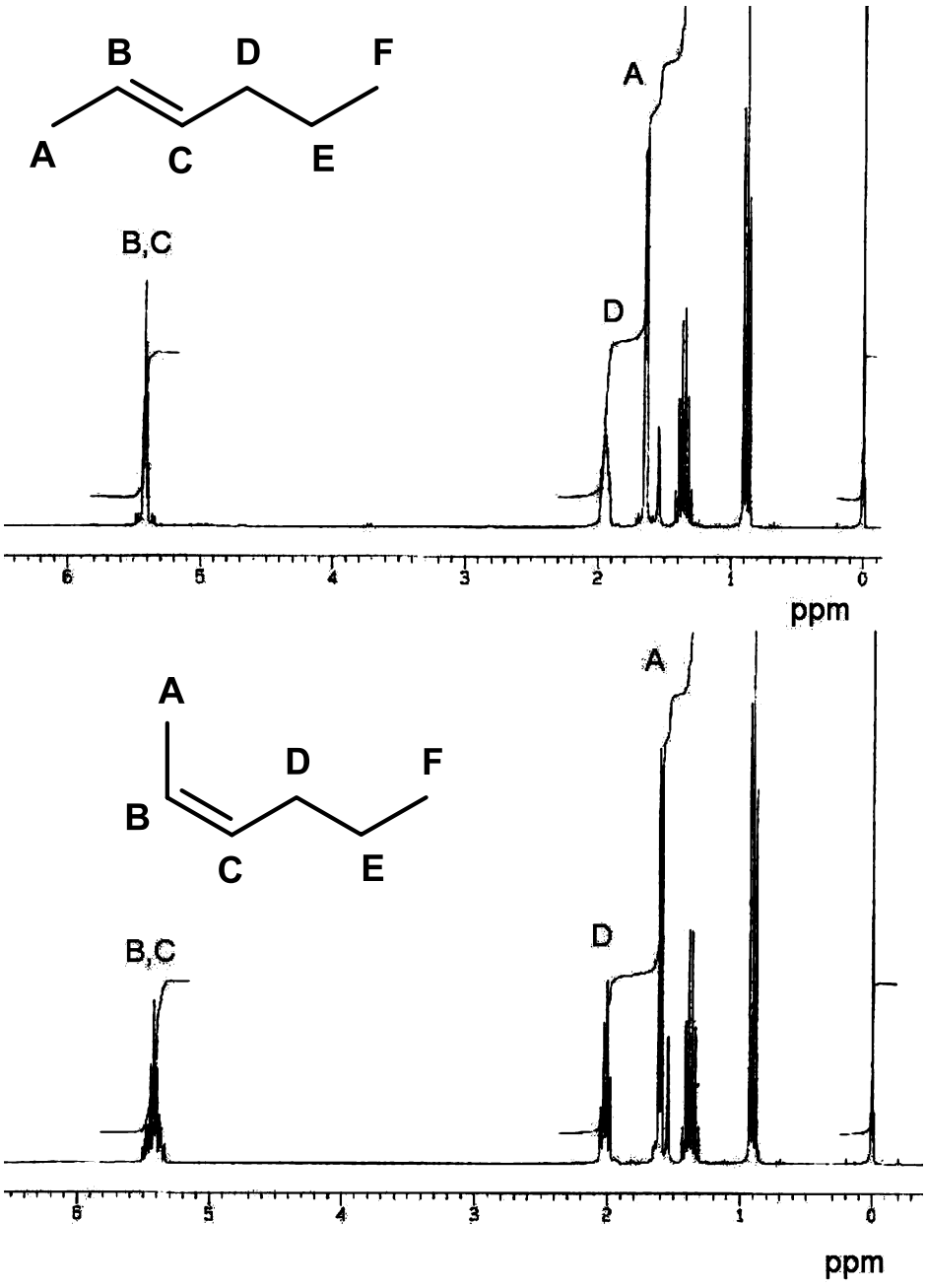

Fig. 4. Comparison of olefinic end groups, ^{1}H-NMR of *E*- and *Z*-isomer.

catalyst **2**, there is a 91:9 favored 2,1-arrangement for the second insertion compared with a 100:0 ratio using catalyst **3**.

With increasing temperature, there is a great increase in the production of dimer **1** and a slight increase for dimers **3** and **4**. Considering the hexene product distribution, we observe a dramatic decrease in the amount of the 2-hexenes (**7** and **8**) and an increase in the amount of 1-hexene (dimer **6**). Catalyst **1** formed only 2% 1-hexene, catalyst **2** had a constant ratio of about 10% and with catalyst **3** the amount of 1-hexene increased up to 20%. In the case of the pentenes, the formation of the terminal vinyl group is more and more favored with an increasing sterical demand shown by comparing the ratios in Fig. 5 for catalyst **1**, Fig. 6 for catalyst **2** and Fig. 7 for catalyst **3**.

When comparing the three catalysts there is clearly a different behavior as shown in Fig. 8. With a slightly higher sterical demand in *ortho* position from a hydrogen to methyl, the dimer distribution dramatically changes. The change from methyl to ethyl on the ligand system does not change the distribution dramatically, but increases the ratio of the 1-olefins.

Considering an even more sterically demanding ligand, one would expect the first 1,2 propylene insertion into the iron hydride to be followed by several 2,1

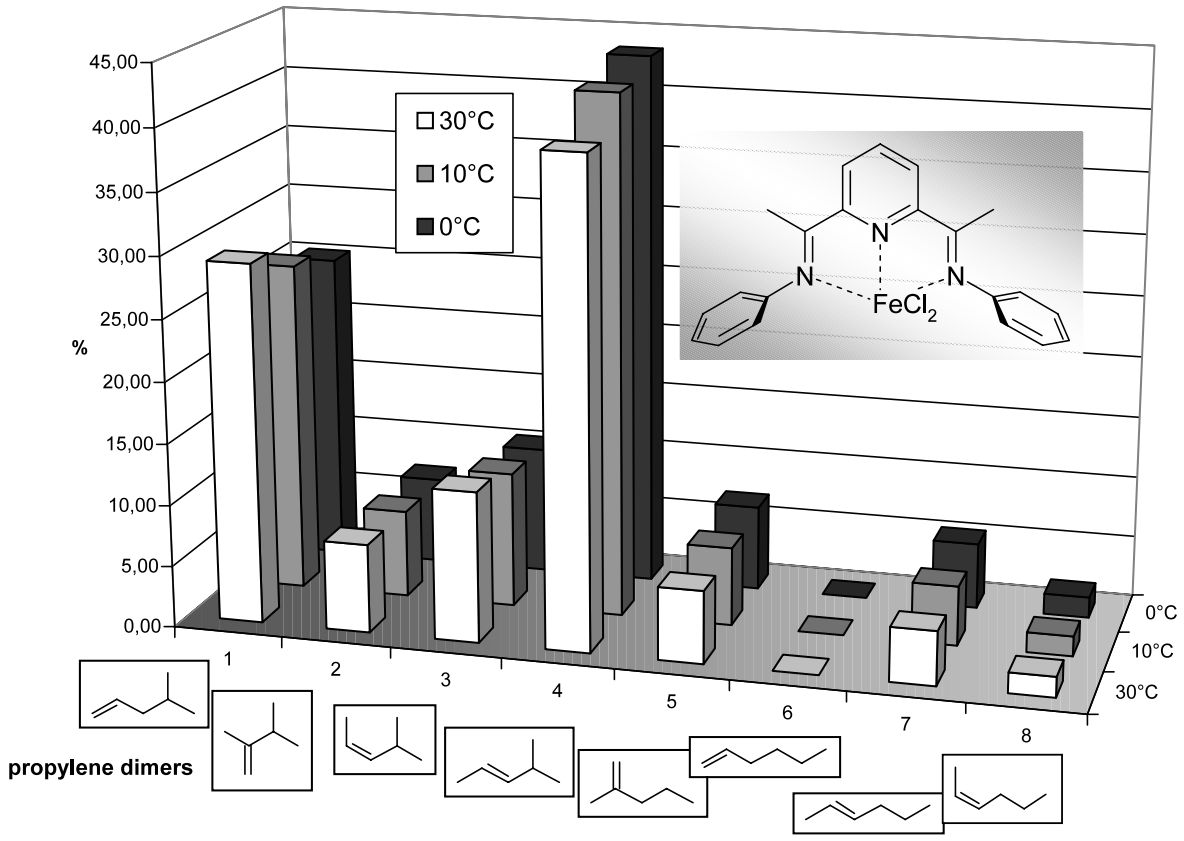

Fig. 5. Propylene dimer distribution of catalyst **1**, propylene bulk phase oligomerization in the Mettler RC1 calorimeter, conditions: [Fe] = 4×10^{-5} mol l^{-1}; 1.5 ml MMAO: [Al] = 3.5×10^{-3} mol l^{-1}; liquid propylene 99.5%; 120 min.

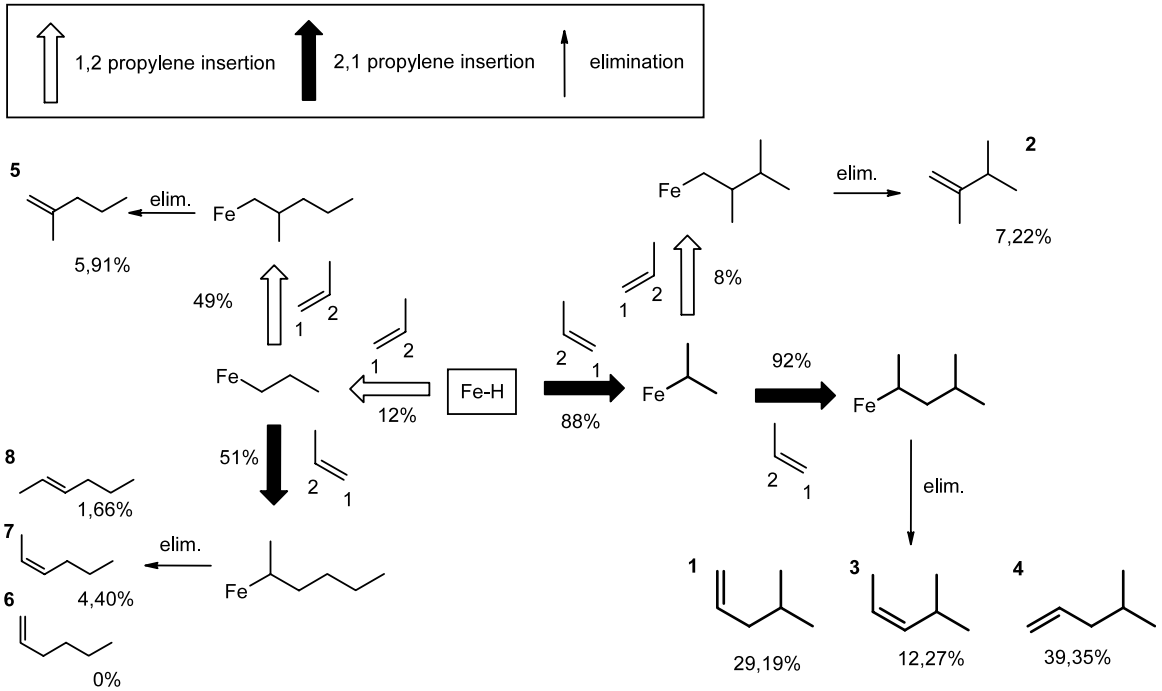

Scheme 1. Mechanism of propylene dimerization with catalyst **1**; propylene bulk phase oligomerization in the Mettler RC1 calorimeter, conditions: [Fe] = 4×10^{-5} mol l^{-1}; 1.5 ml MMAO: [Al] = 3.5×10^{-3} mol l^{-1}; liquid propylene 99.5%; 120 min.

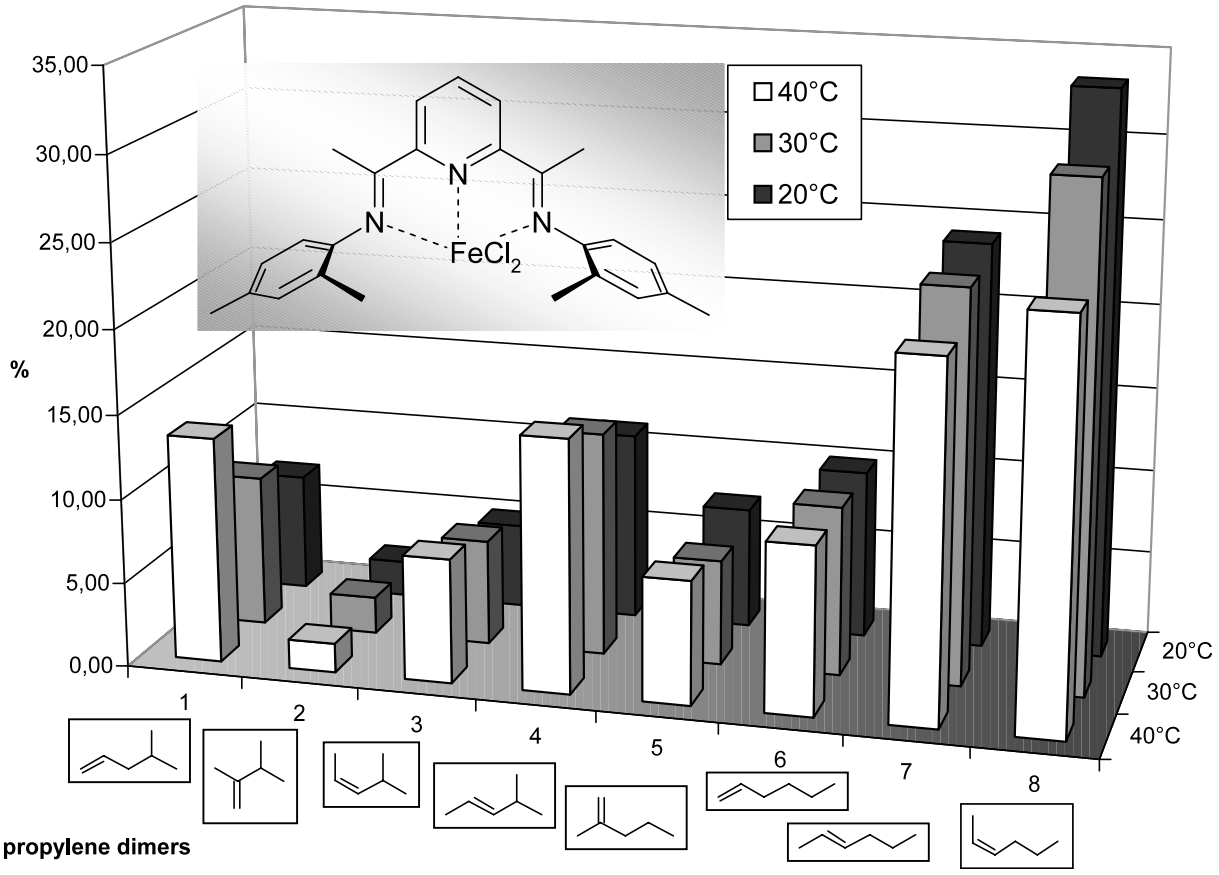

Fig. 6. Propylene dimer distribution of catalyst **2**, propylene bulk phase oligomerization in the Mettler RC1 calorimeter, conditions: [Fe] = 4×10^{-5} mol l^{-1}; 1.5 ml MMAO: [Al] = 3.5×10^{-3} mol l^{-1}; liquid propylene 99.5%; 120 min.

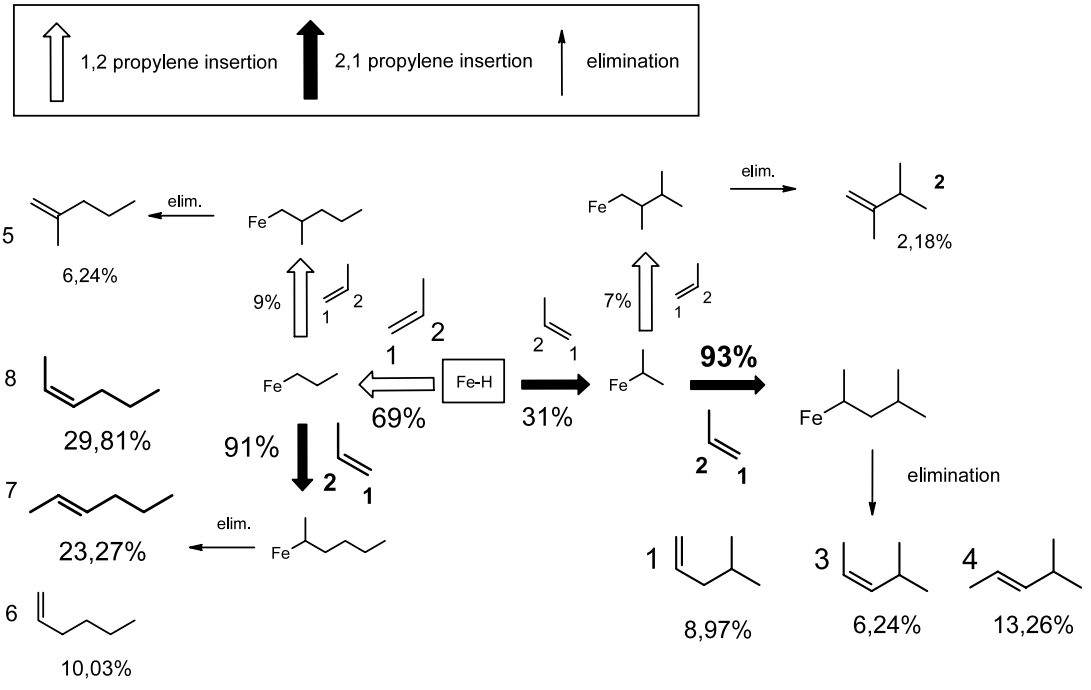

Scheme 2. Mechanism of propylene dimerization with catalyst **2**; propylene bulk phase oligomerization in the Mettler RC1 calorimeter, conditions: [Fe] = 4×10^{-5} mol l^{-1}; 1.5 ml MMAO: [Al] = 3.5×10^{-3} mol l^{-1}; liquid propylene 99.5%; 120 min.

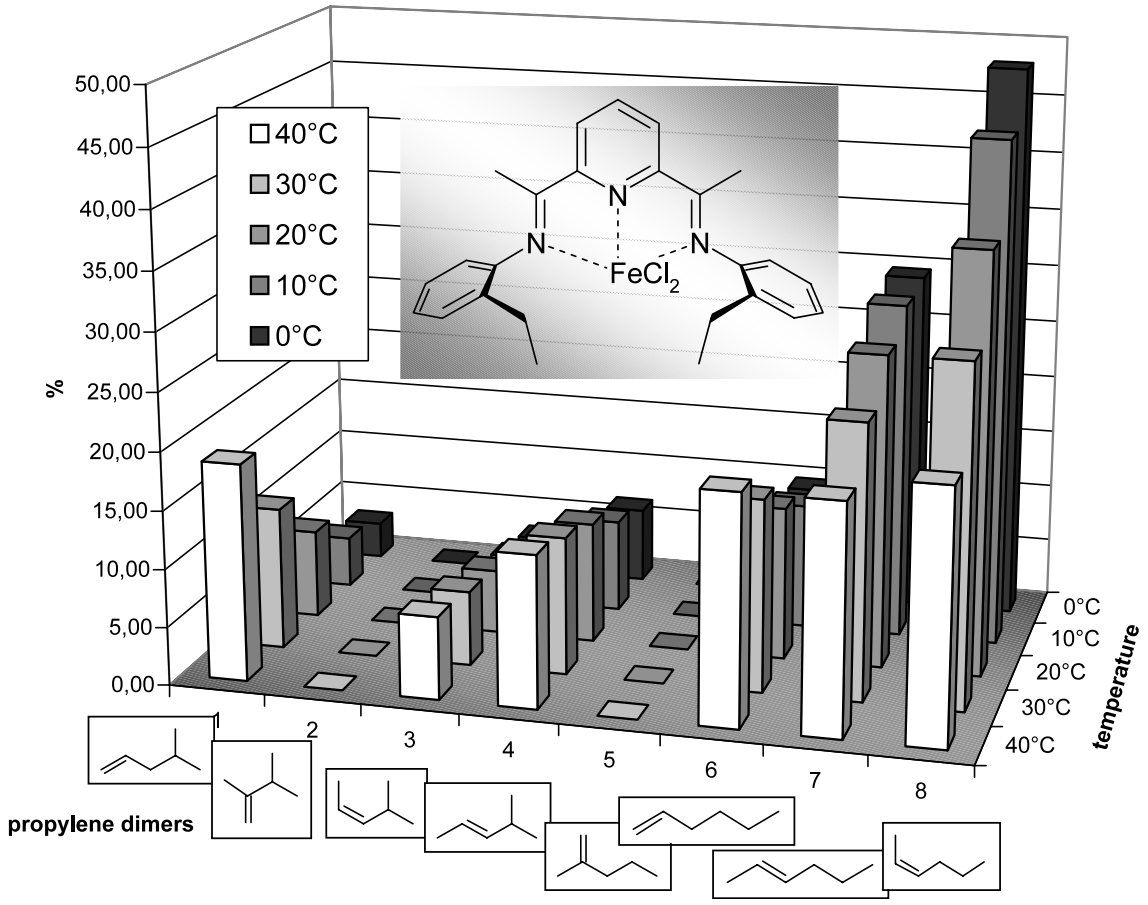

Fig. 7. Propylene dimer distribution of catalyst **3**, propylene bulk phase oligomerization in the Mettler RC1 calorimeter, conditions: [Fe] = 4×10^{-5} mol l^{-1}; 1.5 ml MMAO: [Al] = 3.5×10^{-3} mol l^{-1}; liquid propylene 99.5%; 120 min.

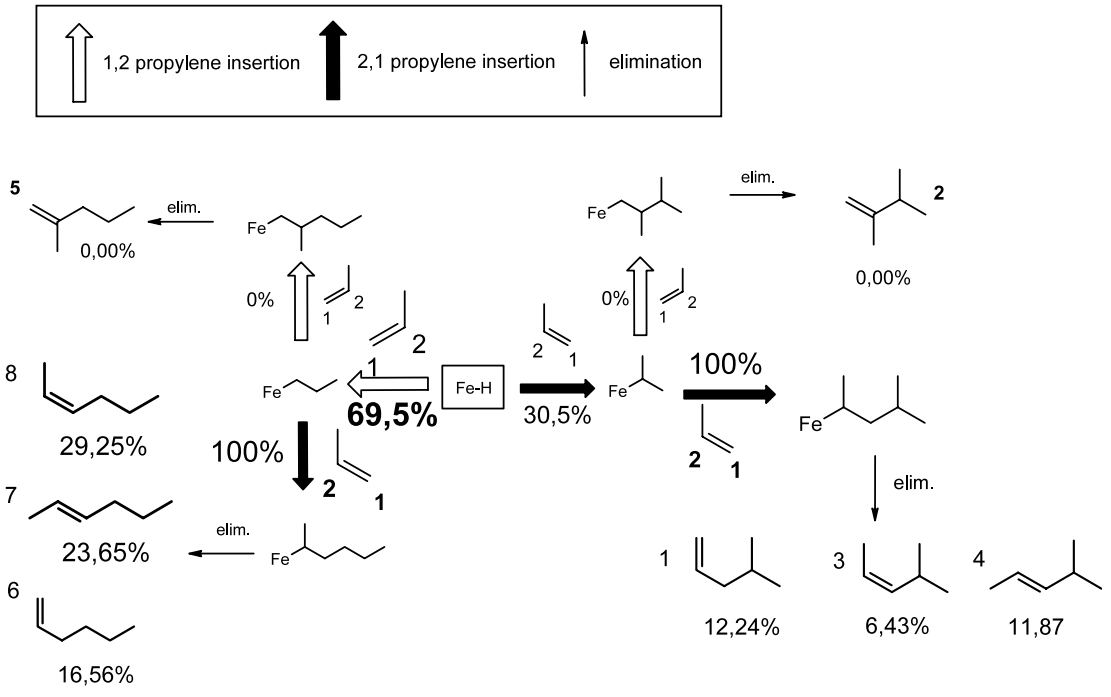

Scheme 3. Mechanism of propylene dimerization with catalyst **3**; propylene bulk phase oligomerization in the Mettler RC1 calorimeter, conditions: [Fe] = 4×10^{-5} mol l^{-1}; 1.5 ml MMAO: [Al] = 3.5×10^{-3} mol l^{-1}; liquid propylene 99.5%; 120 min.

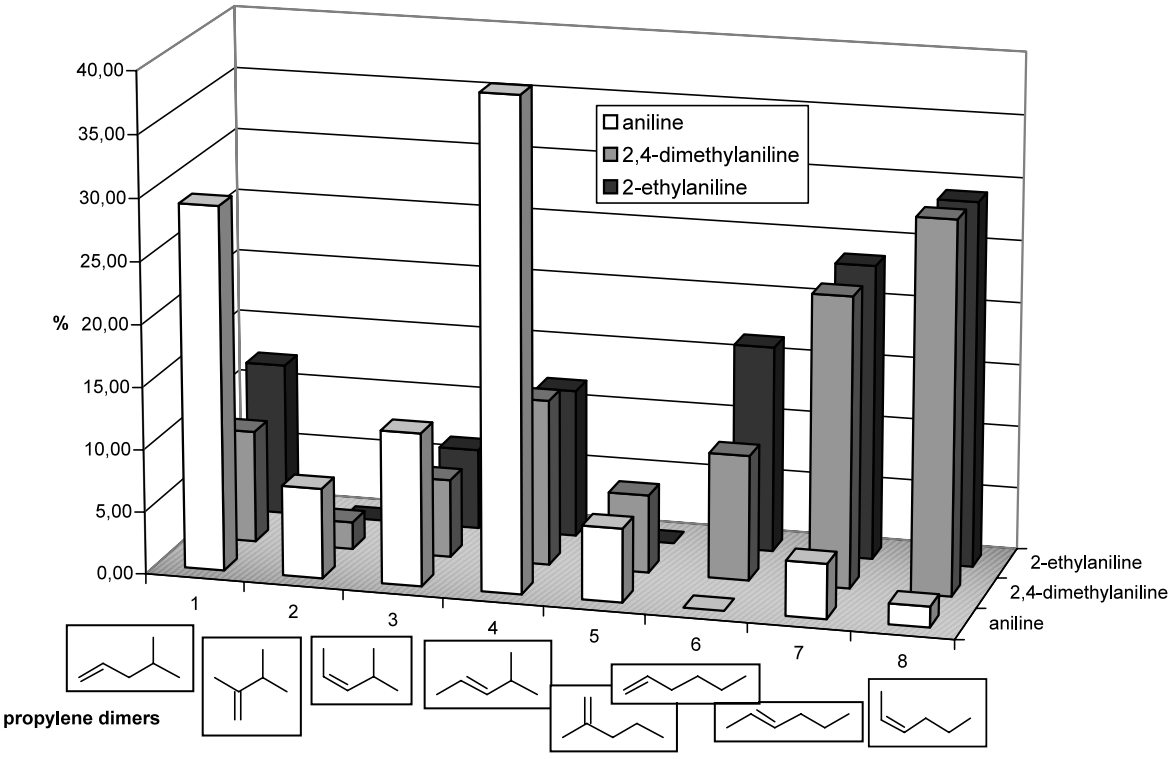

Fig. 8. Propylene dimer distribution with different catalysts **1**–**3**; propylene bulk phase oligomerization in the Mettler RC1 calorimeter, conditions: 30 °C, [Fe] = 4×10^{-5} mol l^{-1}; 1.5 ml MMAO: [Al] = 3.5×10^{-3} mol l^{-1}; liquid propylene 99.5%; 120 min.

insertions. The terminating step should result in a terminal double bond. This is exactly what is observed when a 2-methyl-6-isopropyl substituted catalyst is used [9,17].

Thus far we have concentrated exclusively on the C6 fraction. The percentages for the 1,2 insertion will be much lower, when considering trimers and tetramers. The 2,1 insertions are still involved in the propagation process. Separation of pure trimers by preparative GC was not possible; however, it was possible to identify several trimers with ^{1}H-NMR. Scheme 4 is a mechanistic scheme that includes the trimers and explains which iron alkyls are necessarily to produce the trimers.

In principle we are dealing here with two different iron alkyl species. One is formed after a 1,2 propylene insertion (white arrow) and forms an iron alkyl species with a β-methyl group on the alkyl chain, seen in the upper half in Scheme 4. Because we did not find any of the possible oligomers that might be produced after a propylene insertion in such an iron alkyl, we propose that the elimination is the only possible pathway for these species. The result is the formation of the vinylidene olefin which was isolated with preparative gas chromatography and identified using ^{1}H-NMR.

The other possible iron alkyl species is formed after a 2,1 propylene insertion (black arrow) and results in an iron α-methyl alkyl species. These alkyl species are predominantly responsible for the oligomer or polymer growth. Inserting another propylene molecule in a 2,1-arrangement leads to the same but larger alkyl species and the chain is growing. Insertion in a 1,2-arrangement leads to the β-methyl alkyl species which is a dead end and stops the chain growth.

4. Conclusion

Our approach to the clarification of mechanism was the isolation of oligomers and the identification of the obtained products. Knowing the exact product structure, it is possible to make reasonable approximations on the structure of involved iron alkyl species in the catalytic cycle without identifying the exact alkyl species. With this knowledge we were able to establish a mechanistic scheme for the propylene oligomerization with the bisiminepyridine iron system.

The question of how we produce oligomers versus polymers is a question of knowing how to control the ratio of the 1,2 and 2,1 insertion. One method is to alter the sterical demand in the *ortho* position of the ligand. The more bulky the ligand the more often there happens a 2,1 propylene insertion and therefore higher molecular mass of the oligomer, i.e. polymer. Another important observation is that with a higher sterical demand of the catalysts the formation of the α-olefin is favored. Mechanistic studies contribute to our understanding of polymer reactions and allow greater control of polymer properties, i.e. tailor-made-polymers.

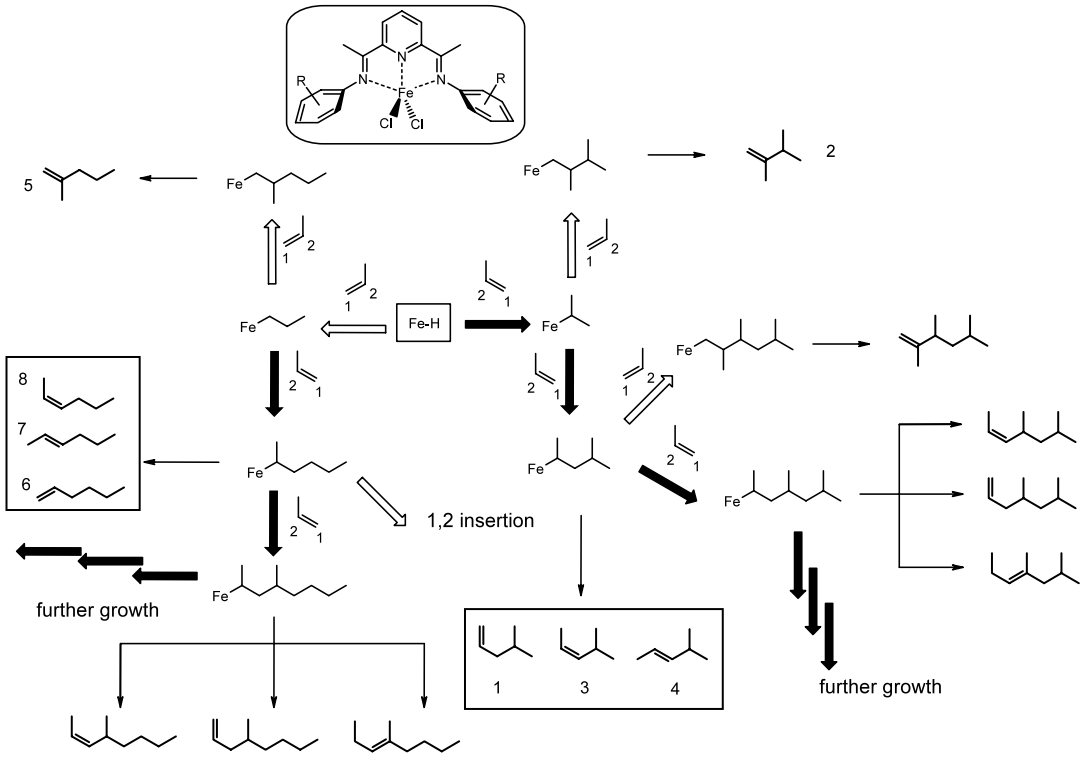

Scheme 4. Mechanism of propylene oligomerization with bisiminepyridine iron complexes in liquid propylene.

5. Outlook

Work that has started but is not completed so far is a combined molecular mechanic/quantum mechanic calculation for several iron alkyls and their energy for the 1,2 or 2,1 propylene insertion. We intend to calculate and visualize the incoming propylene at the iron center. This shall give us an idea how the sterical demand of the ligand effects the processes near the iron center. A visualization of the ligand movement will also give us an idea of how the trajectory of the incoming propylene molecule is hindered by the *ortho* substituents. Another important investigation deals with the nature of the coordination sphere around the iron. We want to know which isomerization steps happen and what the difference in the energy is to switch for example from a growing to a terminating configuration.

References

[1] R.F. Jordan, Adv. Organomet. Chem. 32 (1991) 325.
[2] H.-H. Brintzinger, D. Fischer, R. Mülhaupt, B. Rieger, R. Waymouth, Angew. Chem. 107 (1995) 1255.
[3] K. Soga, T. Shiono, Prog. Polym. Sci. 22 (1997) 1503.
[4] G. Fink, Y. van der Leek, K. Angermund, M. Reffke, R. Kleinschmidt, R. Goretzki, Chem. Eur. J. 3 (1997) 585.
[5] R. Kleinschmidt, Yu. Griebenow, G. Fink, J. Mol. Catal. A: Chem. 157 (2000) 83.
[6] A.u. Wendt, G. Fink, Macromol. Chem. Phys. 202 (2001) 3490.
[7] B.L. Small, M. Brookhart, A.M.A. Bennett, J. Am. Chem. Soc. 120 (1998) 4049.
[8] G.J.P. Britovsek, V.C. Gibson, B.S. Kimberley, P.J. Maddox, S.J. McTavish, G.A. Solan, A.J.P. White, D.J. Williams, Chem. Commun. (1998) 849.
[9] B.L. Small, M. Brookhart, Macromolecules 32 (1999) 2120.
[10] A.M.A. Bennett, Chemtech (1999) 24.
[11] G.J.P. Britovsek, M. Bruce, V.C. Gibson, B.S. Kimberley, P.J. Maddox, S. Mastroianni, S.J. McTavish, C. Redshaw, G.A. Solan, S. Stromberg, A.J.P. White, D.J. Williams, J. Am. Chem. Soc. 121 (1999) 8728.
[12] B.L. Small, M. Brookhart, J. Am. Chem. Soc. 120 (1998) 7143.
[13] G.J.P. Britovsek, S. Mastroianni, G.A. Solan, S.P.D. Baugh, C. Redshaw, V.C. Gibson, A.J.P. White, D.J. Williams, M.R.J. Elsegood, Chem. Eur. J. 6 (2000) 2221.
[14] E.J.M. deBoer, H.H. Deuling, H. van der Heijden, N. Meijboom, A.B. van Oort, A. van Zon, Shell Internationale Research Maatschappij B.V., The Netherlands, PCT Int. Appl. WO 0158874 (2001); Chem. Abstr. 135 (2001) 181084.
[15] E.P. Talzi, D.E. Babushkin, N.V. Semikolenova, V.N. Zudin, V.A. Zakharov–, Kinet. Catal. 42 (2001) 147.
[16] G.J.P. Britovsek, V.C. Gibson, S.K. Spitzmesser, K.P. Tellmann, A.J.P. White, D.J. Williams, J. Chem. Soc. Dalton Trans. (2002) 1159.
[17] S.T. Babik, G. Fink, J. Mol. Catal. 188 (2002) 245.
[18] Alyea, Merrell, Synth. Inorg. Met. Org. Chem. 4 (1974) 535.
[19] F. Korber, K. Hauschild, G. Fink, Macromol. Chem. Phys. 202 (2001) 3329.
[20] F. Korber, K. Hauschild, M. Winter, G. Fink, Macromol. Chem. Phys. 202 (2001) 3323.
[21] Y. Chen, C. Qian, J. Sun, Organometallics 22 (2002) 1231.
[22] L.Q. Deng, P. Margl, T. Ziegler, J. Am. Chem. Soc. 121 (1999) 6479.
[23] D.V. Khoroshen, D.G. Musaev, T. Vreven, K. Morokuma, Organometallics 20 (2001) 2007.